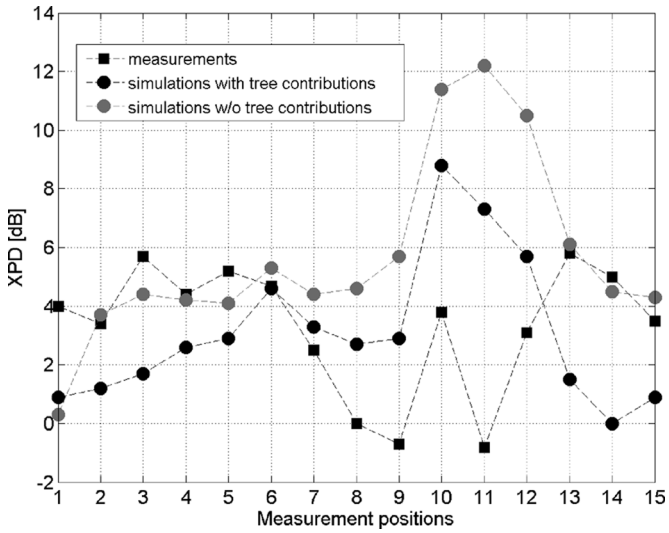

Fig. 4. Comparison of XPD with and without the contribution by trees (scattering and attenuation).

For attenuation, the polarized coefficients presented in [3] help to improve the prediction as the RMSE is reduced to 3.2 dB.

V. Conclusion

In this communication a method to evaluate scattering by tree branches has been presented. This method has been developed to be easily included in a pre-existent 3-D Ray-Tracing tool. The performance of the model is tested with channel measurements in a campus scenario and simulations results are presented.

From this comparison it is possible to conclude that, in such environments, attenuation by vegetation is not sufficient to model tree contribution and that scattering plays a decisive role to correctly evaluate the received power. Scattering is implemented thanks to a reduction coefficient C_r that can be evaluated with respect to the specular reflection with different laws. The results show that when scattering is added to the attenuation, the RMSE may decrease from 6.5 dB to 3.7 dB. The polarization behavior of scattering by trees requires a more detailed study, in order to further improve the XPD prediction.

References

[1] L. Tsang, J. A. Kong, K.-H. Ding, and C. O. Ao, *Scattering of Electromagnetic Waves: Numerical Simulations*. New York: Wiley, 2002.

[2] Y.-C. Lin and K. Sarabandi, "A Monte Carlo coherent scattering model for forest canopies using fractal-generated trees," *IEEE Trans. Geosci. Remote Sensing*, vol. 37, no. 1, pp. 440–451, Jan. 1999.

[3] S. Torrico and R. Lang, "A simplified analytical model to predict the specific attenuation of a tree canopy," *IEEE Trans. Veh. Technol.*, vol. 56, no. 2, pp. 696–703, Mar. 2007.

[4] M. Karam, A. Fung, and Y. Antar, "Electromagnetic wave scattering from some vegetation samples," *IEEE Trans. Geosci. Remote Sensing*, vol. 26, no. 6, pp. 799–808, Nov. 1988.

[5] Y. de Jong and M. Herben, "A tree-scattering model for improved propagation prediction in urban microcells," *IEEE Trans. Veh. Technol.*, vol. 53, no. 2, pp. 503–513, Mar. 2004.

[6] K. L. Chee, S. Torrico, and T. Kurner, "Foliage attenuation over mixed terrains in rural areas for broadband wireless access at 3.5 GHz," *IEEE Trans. Antennas Propag.*, vol. 59, no. 7, pp. 2698–2706, Jul. 2011.

[7] F. Mani and C. Oestges, "Ray-tracing evaluation of diffuse scattering in an outdoor scenario," presented at the 5th Eur. Conf. on Antennas and Propagation—EuCAP, Rome, Italy, Apr. 11–15, 2011.

[8] V. Degli Esposti, F. Fuschini, E. M. Vitucci, and G. Falciasecca, "Measurement and modelling of scattering from buildings," *IEEE Trans. Antennas Propag.*, vol. 55, no. 1, pp. 143–154, Jan. 2007.

[9] D. McNamara, C. Pistorius, and J. Malherbe, *Introduction to the Uniform Geometrical Theory of Diffraction*. Boston, MA: Artech House, 1990.

[10] P. de Matthaeis and R. H. Lang, "Microwave scattering models for cylindrical vegetation components," *Progr. Electromagn. Res.*, vol. 55, pp. 307–333, 2005.

[11] M. A. Weissberger, Final Report Electromagnetic Compatibility Analysis Center, Annapolis, MD, "An Initial Critical Summary of Models for Predicting the Attenuation of Radio Waves by Trees," Tech. Rep., 1982.

[12] ITU-R, "Attenuation in Vegetation," Recommendation ITU-R P.833-4, International Telecommunication Union, Tech. Rep., 1999.

[13] J. Goldhirsh and W. Vogel, "*Handbook of Propagation Effects for Vehicular and Personal Mobile Satellite Systems*," [Online]. Available: http://www.utexas.edu/research/mopro

[14] P. Horak and P. Pechac, "Vegetation Attenuation by a Single Tree for High Elevation Angles at 2.0 and 6.5 GHz," Dept. Electromagnetic Field, Czech Technical Univ., Prague, Tech. Rep..

[15] W. Vogel and J. Goldhirsh, "Earth-satellite tree attenuation at 20 GHz: Foliage effects," *Electron. Lett.*, vol. 29, no. 18, pp. 1640–1641, Sep. 1993.

[16] "Generation of 3D Fractal Trees," [Online]. Available: http://www.mathworks.com/matlabcentral/fileexchange/29537-generation-of-3d-fractal-trees

[17] P. Prusinkiewicz and A. Lindenmayer, "The Algorithmic Beauty of Plants," [Online]. Available: http://algorithmicbotany.org/papers

Legendre Fit to the Reflection Coefficient of a Radiating Rectangular Waveguide Aperture

Dylan F. Williams, Mohammad Tayeb Ghasr, Bradley Alpert, Zhongxiang Shen, Alexander Arsenovic, Robert M. Weikle, II, and Reza Zoughi

***Abstract*—We accurately calculate the reflection coefficient and normalized admittance of radiating open-ended rectangular waveguides and fit our results with a linear combination of Legendre polynomials. We verify the expression to an accuracy of 0.005 with other calculations and examine the impact of flanges and burrs on the accuracy to which the reflection coefficient can be approximated in practice.**

***Index Terms*—Calibration, millimeter-wave, submillimeter wave, terahertz, uncertainty analysis, vector network analyzer.**

I. Introduction

We fit the calculated reflection coefficients and normalized admittances of an infinite radiating open-ended rectangular waveguide to a linear combination of Legendre polynomials, and investigate the accuracy of the Legendre-polynomial expansion when applied to finite waveguide flanges.

Manuscript received October 17, 2011; revised March 05, 2012; accepted March 26, 2012. Date of publication May 23, 2012; date of current version July 31, 2012. This work was supported by the Defense Advanced Research Projects Agency's Terahertz Electronics Program. The views, opinions, and/or findings contained in this article/presentation are those of the author/presenter and should not be interpreted as representing the official views or policies, either expressed or implied, of the Defense Advanced Research Projects Agency or the Department of Defense.

D. F. Williams and B. Alpert are with the National Institute of Standards and Technology, Boulder, CO 80305 USA (e-mail: dylan@ boulder.nist.gov).

M. T. Ghasr and R. Zoughi are with the Missouri University of Science and Technology, Rolla, MO 65409 USA.

Z. Shen is with the School of Electrical and Electronic Engineering, Nanyang Technological University, Singapore 639798, Singapore.

A. Arsenovic and R. M. Weikle II are with the University of Virginia, Charlottesville, VA 22904 USA.

Color versions of one or more of the figures in this communication are available online at http://ieeexplore.ieee.org.

Digital Object Identifier 10.1109/TAP.2012.2201106

Radiating open-ended rectangular waveguides find application in near-field and anechoic antenna measurements [1], as phased-array elements [2]–[4], and in reverberation-chamber measurements. As most rectangular waveguides already have flanges, the impedance of open-ended rectangular waveguides with flanges is of particular interest in these applications. Radiating open-ended rectangular waveguides have also found application in materials measurements [5]. Recently, Liu and Weikle argued in [6] that, because radiating open-ended rectangular waveguides do not suffer from flange misalignment, they may actually be used to set the reference impedance of rectangular-waveguide calibrations more accurately at millimeter-wave and terahertz frequencies than transmission lines and loads. These applications can all benefit from accurate closed-form expressions for the reflection coefficient of radiating open-ended rectangular waveguides. For example, [7] shows how waveguide displacements introduce significant systematic bias into the reference impedance of rectangular-waveguide thru-reflect-line calibrations above 500 GHz, and investigates the use of precision match standards and radiating opens to set the reference impedance of scattering-parameter calibrations.

In this communication, we present a more detailed study of the reflection coefficient of radiating open-ended rectangular-waveguide apertures in infinite half planes and waveguide flanges. We fit a linear combination of Legendre polynomials to calculations from the method of [8] we develop for the reflection coefficient of an open-ended rectangular waveguide radiating into an infinite half space to calculations performed by Ansoft's High-Frequency Structure Simulator[1] (HFSS) and the hybrid calculation method of [9]. We also assess the impact of burrs, pins, and other flange artifacts encountered in practice on the reflection coefficient of a radiating rectangular-waveguide test port with experiments performed in WR 90 and with HFSS simulations, and compare them to the accuracy of our fit.

II. Open-Ended Rectangular Waveguide Radiating Into an Infinite Half Space

Liu and Weikle [6] and Kim, *et al.* [10] estimated the reflection coefficient of open-ended rectangular waveguides from HFSS calculations. However, HFSS is a general-purpose three-dimensional simulator and employs complicated meshing strategies and solution algorithms. As a result, the accuracy of these calculations depends on a number of specific details of the analysis. For example, in HFSS, the grid size, number of iterations, accuracy of the modal input and reference impedance, and distance to perfectly matched layers all affect the accuracy of the calculations, complicating the uncertainty analysis. This in turn makes it difficult to determine the uncertainty of a calibration based on HFSS calculations of the reflection coefficient of radiating test ports used to set the reference impedance of the calibration.

To address this difficulty, we studied the convergence of the mode-matching method of [8] and the hybrid method of [9], when used to determine the reflection coefficient of an open-ended rectangular waveguide radiating into an infinite half space. For this study we used aperture dimensions in the range $b/a \in (0.3, 0.35, \ldots, 0.6)$ and $a/\lambda \in (0.57, 0.6, \ldots, 0.96)$, where b is the height of the waveguide, a is the width of the waveguide, and λ is the free-space wavelength.

Fig. 1 plots the differences between the reflection coefficients obtained from the mode-matching method of [8] with 15 modes and the hybrid method and a reference calculation obtained from the mode-matching method using 28 modes. We plotted the results from [9] in Fig. 1 with respect to one third of the number of modes specified in the program, as the algorithm of [9] does not account for the symmetry of the problem, and includes approximately two unexcited modes for every three modes specified.

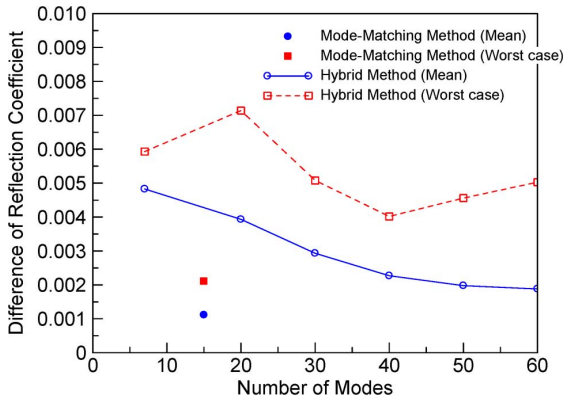

Fig. 1. Differences relative to the mode-matching method using 28 modes.

The figure shows clear convergence of the hybrid method to our reference calculation obtained from the mode-matching approach with 28 modes. The figure also shows that reducing the number of modes in the mode-matching method from 28 to 15 modes had little impact on the result. Based on the figure, we felt that we could expect worst-case errors of no more than 0.005 and mean errors of no more than 0.002 in reflection coefficient if we used our reference calculation based on the method of [8] with 28 modes. Similar considerations led to the adoption of the mode-matching method of [8] in [7].

To speed the calculations, provide useful closed-form expressions, and facilitate comparisons to HFSS simulations, we fit the admittance Y_{open} of rectangular-waveguide opens radiating into a half space as calculated by [8] with 28 modes and [9] with 180 modes specified (approximately 60 equivalent modes) in a least-squares sense to the Legendre-polynomial expansion

$$\frac{Y_{\mathrm{open}}}{Y_0} = \sum_{n=0}^{5}\sum_{m=0}^{7} c_{nm} P_n(q_1) P_m(q_2), \tag{1}$$

where P_n is the Legendre polynomial of order n, $q_1 = -1 + 2(b/a - 0.3)/0.3$, $q_2 = -1 + 2(a/\lambda - 0.57)/0.39$. Here q_1 and q_2 map b/a and a/λ into $[-1, 1]$, the range over which the Legendre polynomials are orthogonal, over the grid spanning $b/a \in (0.3, 0.35, \ldots, 0.6)$ and $a/\lambda \in (0.57, 0.6, \ldots, 0.96)$. We used this polynomial approximation because it is generic and amenable to a linear least-squares solution. Although we also could have fit standard polynomials to the normalized admittance, we chose Legendre polynomials because they improve numerical stability in finite-precision arithmetic. This approach allowed us to determine fitting coefficients for (1) that resulted in the smooth fit to the data shown in the Fig. 2 and reduced the largest residual to only 0.0002. The fitting coefficients we derived from this procedure are given in Table I.

Fig. 2 compares the interpolated values from the mode-matching method of [8] and the hybrid method of [9] to HFSS simulations we performed with perfectly matched layers placed 800 μm from a WM 380 (WR 1.5) [11] aperture of width $a = 380\ \mu$m and a nominal height $b = 190\ \mu$m. The normalized admittances from the mode-matching method of [8] and the hybrid method of [9] deviated by no more than 0.008, which corresponds to deviations of 0.004 in reflection coefficient, from our HFSS calculations, with the largest deviations occurring below the lower end of the waveguide band.

[1]NIST does not endorse commercial products. Product information is only given only to more completely specify the experimental conditions. Other products may work as well or better.

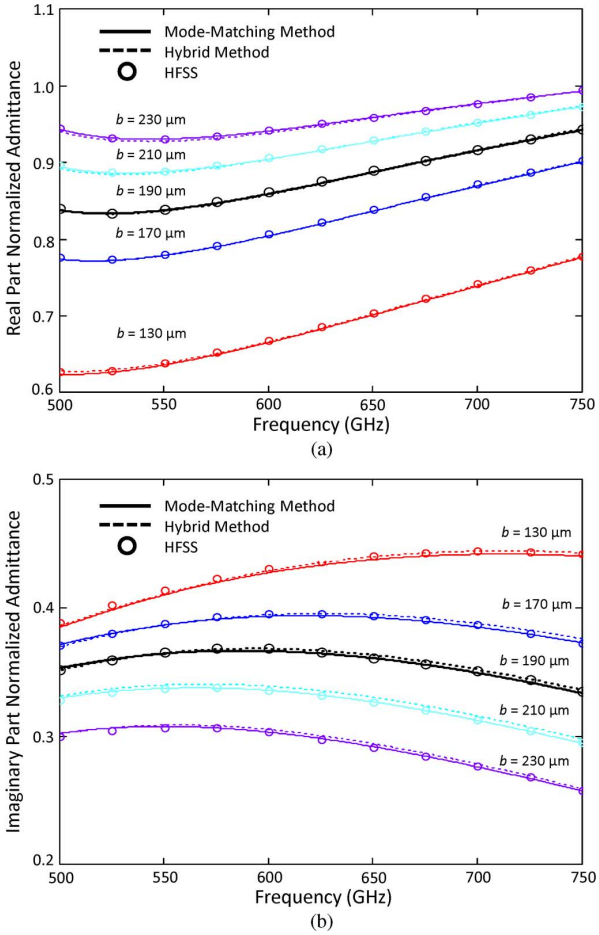

Fig. 2. Comparison of the normalized admittances of open-ended rectangular waveguides radiating into a half space. (a) Real part of normalized admittance. (b) imaginary part of normalized admittance.

III. Measurement Verification

To further verify our Legendre-polynomial fit (1), we fabricated an 8.9 cm by 8.9 cm plate with a WM 2540 (WR 10) aperture in the center. We connected one WM 2540 test port of our vector network analyzer to one face of the plate and performed a thru-reflect-line calibration between the other face of the plate and the second test port of our analyzer, using rectangular waveguide sections of length 0.107 cm, 0.9182 cm, and 1.0233 cm in the calibration. The use of these three lines led to significant redundancy in the calibration.

Figs. 3 and 4 compare our measurements and uncertainties of the magnitude and phase of the reflection coefficient of a WM 2540 (WR 10) aperture radiating into free space to the reflection coefficient estimated from the Legendre-polynomial fit in (1). We placed copper tape over the alignment and screw holes in the plate to reduce their impact.

We found that the level of ripple in the measurements varied greatly with the setup, and changed as we changed the orientation of the radiating aperture with respect to the table and vector network analyzer. From these observations, we concluded that the ripple with a roughly 0.5 GHz period in the measurements is real, and is caused by the finite size of the plate we used and by reflections between the aperture and other elements of the setup.

Nevertheless, we see that the agreement between the measurements and the fit is, in fact, quite reasonable given that we did not perform these measurements in an anechoic chamber where we could have controlled reflections between the radiating aperture and the rest of the apparatus.

We also applied the orthogonal-distance regression algorithm of [12], [13] to estimate our uncertainty in the measurements due to errors in the calibration of the vector network analyzer. This algorithm constructs a Jacobian that maps residuals in the measurements of the redundant calibration standards into estimates of the uncertainties in the calibrated results. To capture test-set drift, we included measurements performed both before and after the measurement of the radiating open in the calibration.

Figs. 3 and 4 show that not all of the discrepancy between the measurements and the polynomial fit can be explained by error in the calibration. We believe that at least some of the remaining differences between our measurements and our Legendre-polynomial fit are probably due to additional close-in reflections between the radiating aperture and our setup, not our calculations.

We also compared our Legendre-polynomial fit to HFSS and CST Microwave Studio1 calculations in [10]. While the magnitudes of the reflection coefficient from (6) of [10] shown in Fig. 3 agree reasonably well with our Legendre-polynomial fit, the uncertainties in our measurements are not low enough to differentiate between the curves. However, we observed that the agreement between the mode-matching method of [8] and the hybrid method of [9] was significantly better than the agreement between those methods and our HFSS calculations, and that the quality of our HFSS calculations depended significantly on the way that the problem was set up. Thus we still have greater confidence in our results.

We also attempted to compare our results to [14], but were not able to obtain the original code required to perform a rigorous comparison. However, we did observe an agreement of 0.005 between our fit to the admittance of a radiating open-ended waveguide and the single-frequency result listed in Table I of [14]. We also note that the authors of [8] and [9] we used to develop our Legendre-polynomial fit did have access to the original code used in [14], and found good agreement between their approaches and the approach of [14] over a broad range of frequencies and dimensions [8], [9].

We also attempted to compare our phase measurements to the fit (7) in [10], but were not able to obtain reasonable results from (7). We suspect that there may be a typographical error in the formula presented in [10], but were not able to confirm this with the authors.

Finally, we compared our results with the measured and analytic reflection coefficients of a flangeless radiating waveguide open reported in [15]. In fact, we found that our Legendre-polynomial fit did not agree well with the analytic expressions and measurements in [15]. However, we used CST Microwave Studio to solve both problems. This study showed that the differences between our results and the measured and analytic reflection coefficients of a flangeless radiating waveguide open reported in [15] were consistent with the difference we would expect from the CST Microwave Studio simulations, further increasing our confidence on our results.

IV. Finite Flanges

Having established a good Legendre-polynomial fit to the reflection coefficient of a rectangular waveguide radiating into an infinite half space, we now turn to the more practical consideration of how well this ideal reflection coefficient models the actual reflection coefficients of radiating opens in flanges having finite dimensions and alignment pins.

A. Pins and Flange

We assessed the impact of reflections from the alignment pins of a UG 387 flange experimentally on the reflection coefficient of a radi-

TABLE I
LEGENDRE-FIT COEFFICIENTS c_{nm} IN (1) DERIVED FROM THE MODE-MATCHING METHOD OF [8] USING 28 MODES

n	m	Real part	Imaginary part
0	0	0.811354817638467	0.373162758714344
1	0	0.170421954885451	-0.0664992345129004
2	0	-0.02649571421256	-0.0151165235446942
3	0	0.000672699763400078	0.00371178887113365
4	0	0.000198111155546295	-0.000269250081103208
5	0	-0.0000361889905335869	-0.0000552529441208527
0	1	0.0568761062294872	0.0115606369197064
1	1	-0.0350562737017482	-0.0388702095962516
2	1	-0.00962682617030087	0.00646372781673429
3	1	0.00151111606855897	0.00125786420100811
4	1	0.0000326987156316627	-0.000417468914785082
5	1	0.0000393050936278311	0.000240473208238237
0	2	0.0386637320869972	-0.0213536099168939
1	2	0.0057512806316703	-0.00118377879382831
2	2	-0.000191592123032103	0.00157487372811151
3	2	0.00042187584139617	-0.000145773444363832
4	2	0.0000468174698693563	0.000263035484179741
5	2	-0.000112240959396222	-0.000382013660792492
0	3	-0.0262007413083819	0.00105050199117572
1	3	-0.00665646513275461	0.00246611909275444
2	3	0.000799886778417885	0.000234427365782445
3	3	0.0000804041487732013	0.000155833609655907
4	3	-0.000141693104285918	-0.00047622464987138
5	3	0.00009372005482889	0.000386652364195411
0	4	0.0119018710260592	0.00133728424576145
1	4	0.00349663118070248	-0.000608134528227083
2	4	-0.000183718314213099	-0.000201867584998731
3	4	-0.0000380409354995906	-0.0000697869762123302
4	4	0.0000152289829669916	0.0000886128055242914
5	4	-0.000041710638760406	-0.000113113010153352
0	5	-0.00523873031599834	-0.000816124307245186
1	5	-0.00147111964860547	0.000342849215472115
2	5	0.0000528863490215359	0.0000370176569034035
3	5	0.0000443352116643522	0.0000884650772831602
4	5	0.0000822839607485526	0.000308881977990892
5	5	-0.000122878538699293	-0.00043219505119681
0	6	0.00245039281375541	0.000409279904893459
1	6	0.000689751098898767	-0.000133940023748766
2	6	-0.0000362346544163783	-0.0000364724980730924
3	6	-0.00000678791397958067	-0.00000236023357179354
4	6	-0.00000621210174532594	-0.0000683031495757776
5	6	0.0000337773039639014	0.000144620344963941
0	7	-0.00104084821157149	-0.000175370825262679
1	7	-0.000314979114296898	-0.0000182445363173592
2	7	0.0000191700663516939	0.0000387929803529162
3	7	-0.0000223380790952549	-0.0000673068689617138
4	7	-0.00000953528990539979	-0.00000535172381170099
5	7	0.0000455278036887788	0.000144858791858804

ating open with scaled WR 90 experiments over the frequency range of 8.2 GHz to 12.4 GHz. Fig. 5 shows the WR 90 aperture and scaled pins we used in the experiments. The sizes and distances of the pins from the aperture were selected to approximate the scaled sizes of pins in waveguide sizes up to WM-380 (WR 1.5), and are shown in their actual positions in the figure. While the pins must be placed farther from the aperture as the frequency is scaled upwards, they also become larger, resulting in a slower decay than might be expected.

We then fit our measured results to the radar cross section of a cylinder, and added in a term to account for large reflections we observed when the pin was in the near field of the aperture. This resulted in the rough approximation

$$|\Delta\Gamma_{\rm pin}| \sim 0.018\sqrt{\frac{h_{\rm pin}\, r_{\rm pin}}{R^2}\frac{h_{\rm pin}}{\lambda_0}\left(\left(\frac{\lambda_0}{R}\right)^2 + 60\left(\frac{\lambda_0}{R}\right)^5\right)} \quad (2)$$

for the average impact $\Delta\Gamma_{\rm pin}$ on the reflection coefficient of the radiating open, where $h_{\rm pin}$ is the height of the alignment pin, $r_{\rm pin}$ is its

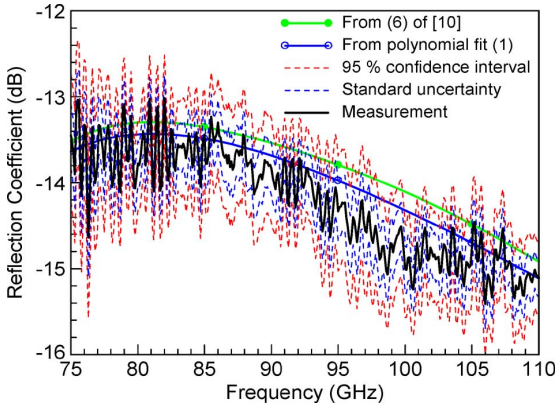

Fig. 3. Magnitude of the reflection coefficient of radiating open-ended waveguide with an infinite and semi-infinite flange.

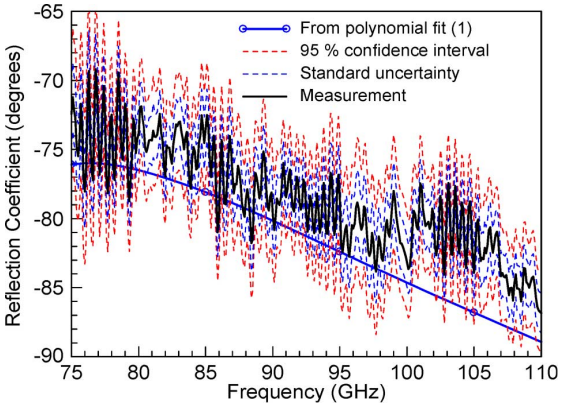

Fig. 4. Phase of the reflection coefficient of radiating open-ended waveguide with an infinite and semi-infinite flange. Estimates of the phase from [10] were not available for comparison (see discussion).

Fig. 5. WR 90 aperture and scale-model pins.

radius, R is the distance between the center of the aperture and the pin, and λ_0 is the free-space wavelength.

The first term in (2) corresponds to the radar cross section of a cylinder in the far field. This term is most significant at millimeter wavelengths, as it decays slowly with frequency. The second term dominates at lower frequencies, and leads to large reflections in larger waveguide sizes used at lower frequencies.

Finally, we built an HFSS model for the UG 387 flanges we used. The model included the pins, the holes for the screws, the boss specified in [16], and the edge of the flange. We were unable to run the HFSS simulations in the far field of the aperture because the problem size became too large for our computers. However, we were able to run the

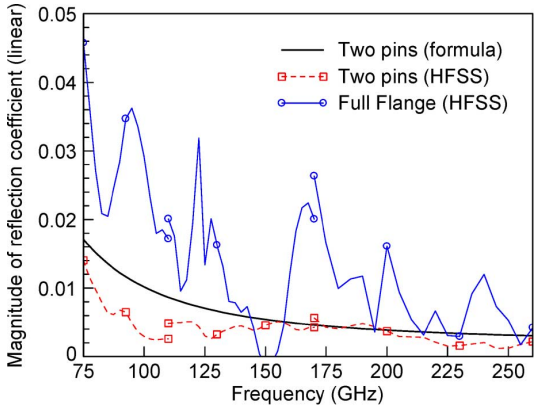

Fig. 6. Comparison of HFSS simulations to the experimentally based formula (2).

simulations for WM-2540 (WR 10), WM-1650 (WR 6) and WM-710 (WR 4) openings in the flange.

Fig. 6 compares the experimentally-based formula (2) for two pins in a UG 387 flange with $h_{\rm pin} = 3.96$ mm, $r_{\rm pin} = 0.813$ mm and $R = 7.144$ mm to our HFSS calculations. The agreement between (2) and the HFSS calculation of the reflection off two pins is only fair, but agrees reasonably well with (2). The HFSS calculations for the reflection off the entire flange marked with circles in Fig. 6 indicate that (2) underestimates the reflection off other flange components by as much as a factor of three or four.

Thus we multiplied (2) by a factor of 6 before incorporating it into the error analysis of [7]. The first factor of two accounted for the fact that we had two pins on each flange, and the factor of 3 accounted for the best estimate we had available for the additional impact of the boss and edge of the flange on the reflection coefficient of our radiating opens.

Finally, we note that our estimated uncertainty of 0.002 in our Legendre-polynomial fit does not become comparable to $2|\Delta\Gamma_{\rm pin}|$ calculated from (2) for a UG 387 flange until about 100 THz. This indicates that the accuracy of our Legendre-polynomial fit is more than adequate at terahertz frequencies, and that reflections from the pins and flanges more seriously limit calibration accuracy.

B. Burrs

We also used HFSS to develop the rough approximation

$$\Delta\Gamma_{\rm open} \approx -6\left[\left(\frac{h}{a}\right)^2 + 1000\left(\frac{h}{a}\right)^6\right]\left[\cos\left(\pi\frac{y}{a}\right) + 2i\cos\left(\frac{4\pi}{3}\frac{y}{a}\right)\right] \quad (3)$$

for the change $\Delta\Gamma_{\rm open}$ in the refection coefficient of a radiating open due to a burr of dimension h and position y on the broad wall of the test-port aperture. Appendix I of [7] presents a similar formula for burrs at the interface between two rectangular waveguides. Our simulations indicated that burrs on the narrow wall of the aperture had a much smaller impact on reflections, and we neglected these burrs in our analysis.

Equation (3) indicates that the impact of burrs grows with increasing frequency, and that even burrs as small as 2.5 μm have as much impact on the reflection coefficient of a radiating open at 1 THz as the 0.002 uncertainty in our Legendre-polynomial fit to the reflection coefficient of a radiating open.

V. Software

We have encapsulated the results of this analysis in the freeware packages [17] and [18].

VI. Conclusion

We fit a linear combination of Legendre polynomials to the reflection coefficient of open-ended rectangular waveguides radiating into an infinite half space to an accuracy of approximately 0.002. Our analysis indicates that reflections from the pins, edges, and burrs of UG 387 flanges are large enough that this error in the Legendre-polynomial fit can be ignored in practice. The analysis also provides a firm basis for the uncertainty analysis described in [7].

Acknowledgment

The authors thank R. Direen for assistance with the measurements.

References

[1] M. Kanda and R. D. Orr, "Near-filed gain of a horn and an open-ended waveguide: Comparison between theory and experiment," *IEEE Trans. Antennas Propag.*, vol. AP-35, no. 1, pp. 33–40, Jan. 1987.

[2] R. J. Mailloux, "Radiation and near-field coupling between two collinear open-ended waveguides," *IEEE Trans. Antennas Propag.*, vol. AP-17, no. 1, pp. 49–55, Jan. 1969.

[3] Y. Rahmat-Samii, P. Cramer, K. Woo, and S. W. Lee, "Realizable feed-element patterns for multibeam reflector antenna analysis," *IEEE Trans. Antennas Propag.*, vol. AP-29, no. 6, pp. 961–963, Jan. 1981.

[4] S. W. Lee and M. L. Zimmerman, "Reflector spillover loss of an open-ended rectangular and circular waveguide feed," *IEEE Trans. Antennas Propag.*, vol. 38, no. 6, pp. 940–942, Jan. 1990.

[5] V. Theodoris, T. Sphicopoulos, and F. E. Gardiol, "The reflection from an open-ended waveguide terminated by a layered dielectric medium," *IEEE Trans. Microwave Theory Tech.*, vol. MTT-33, pp. 359–366, May 1985.

[6] Z. Liu and R. M. Weikle, "A reflectometer calibration method resistant to waveguide flange misalignment," *IEEE Trans. Microwave Theory Tech.*, vol. 54, no. 6, pp. 2447–2452, Jun. 2006.

[7] D. F. Williams, "500 GHz–750 GHz rectangular-waveguide vector-network-analyzer calibrations," *IEEE Trans. Terahertz Sci. Technol.*, Nov. 2010.

[8] M. T. Ghasr, D. Simms, and R. Zoughi, "Multimodal solution for a waveguide radiating into multilayered structures-dielectric property and thickness evaluation," *IEEE Trans. Instrum. Meas.*, vol. 58, no. 5, pp. 1505–1513, May 2009.

[9] B. Zheng and Z. Shen, "Analysis of dielectric-loaded waveguide slot antennas by the hybrid mode-matching/moment method," *IEICE Trans. Commun.*, vol. E88-B, no. 8, pp. 3416–3427, Aug. 2005.

[10] J. H. Kim, B. Enkhbayar, J. H. Gang, B. C. Ahn, and E. J. Cha, "New formula for the reflection coefficient of an open-ended rectangular waveguide with or without an infinite flange," *PIERS*, vol. 12, pp. 143–153, ISSN: 1937-8726.

[11] N. M. Ridler, R. A. Ginley, J. L. Hesler, A. R. Kerr, R. D. Pollard, and D. F. Williams, "Towards standardized waveguide sizes and interfaces for submillimeter wavelengths," presented at the 21st Int. Symp. Space Terahertz Technology, Mar. 2010.

[12] D. F. Williams, C. M. Wang, and U. Arz, "An optimal vector-network-analyzer calibration algorithm," *IEEE Trans. Microw. Theory Tech.*, vol. 51, no. 12, pp. 2391–2401, Dec. 2003.

[13] D. F. Williams, C. M. Wang, and U. Arz, "An optimal multiline TRL calibration algorithm," in *roc. IEEE MTT-S Int. Microwave Symp. Dig.*, Jun. 2003, vol. 3, pp. 1819–1822.

[14] R. H. MacPhie and A. I. Zaghloul, "Radiation from a rectangular waveguide with infinite flange-Exact solution by the correlation matrix method," *IEEE Trans. Antennas Propag.*, vol. 28, no. 4, pp. 497–503, Jul. 1980.

[15] K. T. Selvan and V. Venkatesan, "A note on the aperture-reflection coefficient of open-ended rectangular waveguide," *IEEE Trans. Electromagn. Compatibility*, vol. 45, no. 4, pp. 663–664, Nov. 2003.

[16] J. L. Hesler, A. R. Kerr, W. Grammer, and E. Wollack, "Recommendations for waveguide interfaces to 1 THz," in *18th Int. Symp. Space Terahertz Technology*, Mar. 2007, pp. 100–103.

[17] D. F. Williams, Rectangular-Waveguide Calculator National Institute of Standards and Technology [Online]. Available: http://www.boulder.nist.gov/dylan, 2010

[18] D. F. Williams and A. Lewandowski, NIST Microwave Uncertainty Framework National Institute of Standards and Technology [Online]. Available: http://www.boulder.nist.gov/dylan, 2011

Statistical Analysis for On-Body Spatial Diversity Communications at 2.45 GHz

Asimina Michalopoulou, Antonis A. Alexandridis, Kostas Peppas, Theodore Zervos, Fotis Lazarakis, Kostas Dangakis, and Dimitra I. Kaklamani

***Abstract*—An investigation of the fading experienced by on-body diversity channels at 2.45 GHz is presented by focusing on the effects of the receive antennas position and the human body movement. This investigation is based on the conduction and analysis of signal measurements in an indoor office environment using bodyworn antennas. Three principal combining techniques, namely selection combining (SC), equal gain combining (EGC) and maximal ratio combining (MRC) are considered. A statistical characterization of the fading experienced by dual diversity on-body channels is performed in terms of first and second order statistics. Our investigations have shown that among several distributions tested, the $\alpha - \mu$ distribution provides sufficient fit to measured combined signal envelopes and also offers a good approximation to second order statistics for the majority of test cases.**

***Index Terms*—Body area network (BAN), channel modeling, diversity, on-body channel, propagation measurements, second order statistics.**

I. Introduction

Recently the decreasing size of wearable devices and the proliferation of applications implementing wearable systems have significantly raised the interest of the research community in on-body communications. Currently, on-body communications are under standardization by the IEEE 802.15.6 body area network (BAN) group [1] regarding several application areas such as medical, military, personal recreation and more. Recent BAN implementations, such as military and sport equipment for communications between wearable transceivers demonstrate the ever increasing need for systems with higher data rate and larger system throughput [2]. At the same time, on-body channels are subject to a continuously variable environment caused by changes in body posture, surrounding environment and signal direction. Furthermore, the transmitted power levels should be relatively low. Under these circumstances, spatial diversity could be used to mitigate fading and increase communication rates in an on-body environment.

A critical issue for a successful BAN system design is the accurate statistical modeling of the propagation channel. In the past, a significant

Manuscript received March 03, 2011; revised March 01, 2012; accepted March 09, 2012. Date of publication May 22, 2012; date of current version July 31, 2012.

A. Michalopoulou is with the Institute of Informatics and Telecommunications, NCSR "Demokritos", GR 15310 Athens, Greece and also with the School of Electrical and Computer Engineering, National Technical University, GR 15773 Athens, Greece (e-mail: asimihal@iit.demokritos.gr).

A. A. Alexandridis, K. Peppas, T. Zervos, F. Lazarakis and K. Dangakis are with the Institute of Informatics and Telecommunications, NCSR "Demokritos", GR 15310 Athens, Greece (e-mail: aalex@iit.demokritos.gr; kpeppas@iit.demokritos.gr; tzervos@iit.demokritos.gr; flaz@iit.demokritos.gr; kdang@iit.demokritos.gr).

D. I. Kaklamani is with the School of Electrical and Computer Engineering, National Technical University, GR 15773 Athens, Greece (e-mail: dkaklam@mail.ntua.gr).

Digital Object Identifier 10.1109/TAP.2012.2201073